COMPARISON OF LAB & FIELD CALIBRATION METHODS OF A DIGITAL NON METRIC CAMERA FOR UAV-PHOTOGRAMMETRY LOW-COST APPLICATIONS

M. Pérez [a], F. Agüera [a], F. Carvajal [a],

[a] ESI - Dept. of Rural Engineering, University of Almeria, Crta. Sacramento sn, 04120 Almeria, Spain – mps515@ual.es

KEY WORDS: Unmanned Aerial Vehicle, digital non-metric camera, camera calibration, UAV photogrammetry, Photomodeler Scanner software

ABSTRACT:

Digital cameras are becoming available with many smaller formats capable of precise measurement applications. They require calibration to determine their metric characteristics in order to carrying out photogrammetric activities. For more accurate results, the calibration images should be taken under similar conditions to the field samples.

The aim of this work was to compare a standard methodology used by Photomodeler Scanner software for lab calibration using a low cost non-metric camera with a camera calibration made in the environmental conditions and the surface to be modelled. Within field calibration we compared three methods: field calibration 1 was done with only automatic autocorrelated points, field calibration 2 had automatic points and points introduced manually and field calibration 3 was carried out with only manual points. To achieve this goal, low cost equipment and software were used.

First, lab calibration was done using a grid pattern obtained from EOS Systems Inc. The focal length was fixed at widest angle and the network included twelve images with ± 90º roll angles. To develop the field calibration, a flight planning was programmed including fourteen images. To carry out the flight an unmanned aerial vehicle (UAV) was used. In the same way as in the lab calibration, the focal length was fixed at widest angle. The altitude flight over ground was 50 m. The field test used in the study was a surface located in Almería (Spain) and a set of 29 target points were placed. These points were used as ground control points (GPC) and as check points in the different projects carried out. The calibrated parameters obtained were focal length (only in lab calibration), the format size of the CCD sensor (only in lab calibration), the principal point coordinates, radial lens distortions and decentring distortions. The chosen error estimator was the well-known root mean squared error (RMS) based on the 29 target points set. The RMSs obtained had the same magnitude order. It was concluded that in our photogrammetric applications maybe we can avoid a very strict surveying of GCP to the block adjustment, if we use the automatic autocorrelation algorithm to obtain the tie points. The lab calibration was carried out once in order to characterize the interior orientation parameters (IOP) and then it was used as pre-calibration in all field calibration methods.

1. INTRODUCTION

Digital cameras are becoming available with many smaller formats capable of precise measurement applications. They require calibration to determine their metric characteristics in order to carrying out photogrammetric activities (Habib and Morgan, 2003). A common criticism with small format aerial photography is the camera's geometric instability and limited precision and accuracy (Warner and Carson 1991). This criticism becomes even more significant with digital cameras and their low-cost lenses. Often, it is impossible to obtain data about the interior orientation of the camera; thus, alternative camera calibration methods have been suggested (Zhang, 2000). The use of low cost digital photogrammetric systems like Photomodeler has contributed to the use of these "off the shelf" cameras among photogrammetrist and non photogrammetrist (Cardenal et. al., 2004).

Camera parameters commonly discovered through calibration procedures include the computed principal distance or focal length *(f)* of the lens, parameters (x_p, y_p) which denote the coordinates of the centre of projection of the image (principal point), and lens distortion coefficients *(k1, k2, k3, p1, p2, p3)* where the terms *ki* represent coefficients of radial lens distortion and *pi* terms represent coefficients of decentring distortion caused by a lack of centring of lens elements (William, 2005). Radial and decentring distortions comprise the aberrations which affect the location of images (Fryer, 1996).

Many calibration techniques have been developed in the last few years: Mason et al. (1997), Karras and Mavrommati (2001), Honkavaara et al. (2006), Remondino and Fraser, (2006), Douskos et al. (2007), Grammatikopoulos et al. (2007), Wang et al. (2008), Zhang et al. (2010) and others, but there are not many calibration techniques in which the images are taken from UAVs. The evolution of techniques for determining lens distortion can be shown in Clarke and Fryer (1998).

The success of digital camera calibration establishes the prerequisite and foundation for digital close-range photogrammetry and 3D modelling (Zhang et al. 2010). In situ calibrations are characteristic for close range applications: camera calibration and object reconstruction is done within one process named simultaneous calibration (Cramer, 2004).

Field calibration uses terrestrial features which have been surveyed to relatively high degree of accuracy to calibrate camera lenses. The advantages of this method are the accuracy of these points, which have typically been surveyed previously; the fact that the camera can be used in conditions similar to which it will operate; and calibration can take place at a similar time to use (Clarke and Fryer, 1998).

In recent years, Unamanned Aerial Vehicles (UAVs) have demonstrated their great potential for photogrammetric measurements in many application fields. UAV photogrammetry (Colomina et al., 2008) indeed opens various new applications in the close-range domain and introduces also low-cost alternatives to the classical manned aerial photogrammetry (Eisenbeiss, 2009). According to Colomina et.

al. (2008), UAVs are a new paradigm for high-resolution low-cost photogrammetry and remote sensing, especially given the fact that consumer non digital cameras provide a sufficiently high accuracy for many photogrammetric tasks (Gruen and Akca, 2008).
The main advantage of an UAV system acting as a photogrammetric sensor platform over more traditional manned airborne or terrestrial surveys is the high flexibility that allows image acquisition from unconventional viewpoints (Irschara et al. 2010).
The aim of this work was to compare a standard methodology used by Photomodeler software for camera calibration using a low-cost non-metric camera with a camera calibration made with Photomodeler too, but in the environmental conditions and the surface to be modelled. The camera calibration techniques described in this paper were used with the consideration of robustness, flexibility and low-cost.

2. MATERIALS AND METHODS

2.1 Camera platform and image acquisition

A Pentax Optio A40 digital camera was mounted on UAV manufactured by Microdrones, the md4-200 (http://www.microdrones.com), to take images of a surface located in Almeria, (Spain). The camera can be tilted to capture images from different angles and it has 12.0 mega pixels resolution, picture stabilization, trigger and zoom function. The md4-200 can be programmed to follow a route defined by several way-points and actions. It has the ability for vertical take off and landing with autonomous and semiautonomous control capacities, provides position hold and autonomous way-point navigation, with GPS antenna, altimeter and magnetometer to calculate the position coordinates during the flight (see Fig. 1).

Figure 1. Md4-200 with the digital camera Pentax Optio A40

The drone can be operated fully autonomous including auto start and auto landing, thanks to the waypoint navigation guidance. In our work the take off and the landing were manual and the rest of the flight was autonomous.

2.2 Flight Planning

The flight planning was programmed using the Md-Cockpit V2.6.2.6 compatible software with the drone. Using the module Waypoint Editor, the flight path was designed. It is a graphical interface based on Google Earth information, and the actions to do in each waypoint were defined, including holding position, picture orientation and trigger activation.
For field calibration a route was defined including a total of 14 waypoints (see Fig. 2). Each waypoint had assigned the action of taking a photo.

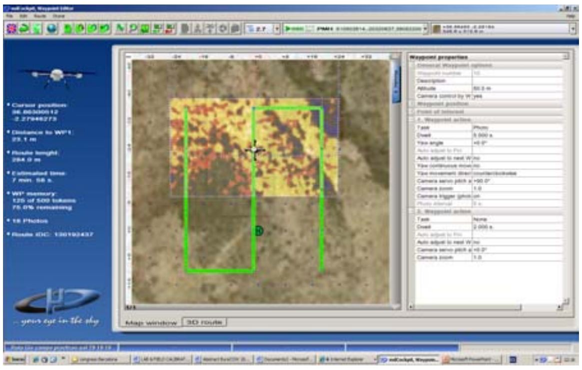

Figure 2. Flight planning with Md-Cockpit V2.6.2.6

2.3 Digital camera calibration methods

Camera calibration was accomplished using Photomodeler Scanner software. The focal length, the coordinates of the principal point and the radial lens distortion parameters were estimated via bundle adjustment.
In this study different camera calibration methods were done. The first one consists in a lab calibration with a planar pattern and the others, field calibrations made in the environmental conditions and the surface to be modelled. In all methods the software Photomodeler Scanner was used to find out the interior parameters.

2.3.1 Lab camera calibration. In June 2010 a set of 12 convergent images covering the calibration pattern included in the installation package of Photomodeler Scanner were taken. The pattern was placed on the floor and three images were collected from each of the pattern's four sides. Figure 3 shows some of the images taken from the calibration pattern attached on the floor. A tripod was used to ensure image stability. For good calibration results with the lab calibration method, images should cover the whole imaging area and should be of very good sharpness and contrast. Also a minimum of eight images with good convergent positions are required (www.photomodeler.com).

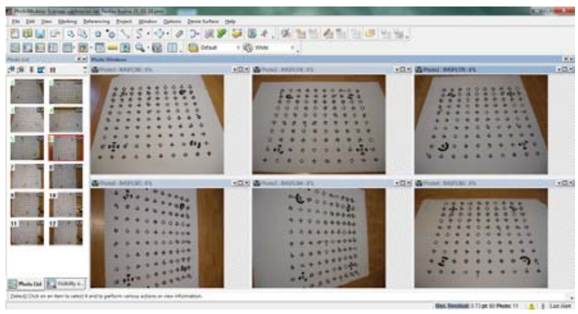

Figure 3. Calibration pattern used for lab camera calibration

The focal length was fixed at minimum zoom (widest angle) and the network included images with ± 90º roll angles. The camera positions were close to 45 degrees from the horizontal and vertical.
Interior orientation parameters (IOP) of the digital camera were estimated using the module Camera Calibrator of Photomodeler Scanner software in which the bundle block adjustment method is used. Image point detection was automatically done and the calibration results were stored.
The lab calibration was carried out once to calculate the IOP but in all field applications, a field calibration was applied using the lab calibration results as initial parameters.

2.3.2. Field camera calibrations. The calibration images should be taken under similar conditions to the field samples for most accurate results. In order to get this goal, we proposed a camera field calibration using an UAV to take the images under similar conditions as our future photogrammetric projects.

To develop the field calibration, as it is mentioned above, a flight planning was programmed defining a route including a total of 14 vertical images. In the same way as with lab calibration, the focal length was fixed at the widest angle and recorded as a 3648 by 2736 pixels image. The test-field used in the study was a non flat surface located in Almeria (Spain) and a set of 29 black and white target points covering the calibration test-field were used. The test-field used in this work covered a surface of 7.000 m^2 approximately. Within field calibration we compared three methods: field calibration 1 was done with only automatic autocorrelated points, field calibration 2 had automatic points and points introduced manually and field calibration 3 was carrying out with only manual points. For these methods, the focal length and the format size parameters were assumed to be the same as the obtained in lab calibration. The three-dimensional coordinates of the 29 target points were determined with a GPS Trimble R6. The altitude flight over ground was 50 m. For field calibration 1, an automated project choosing the option SmartPoints project (non-target feature points) was set up using the lab calibration internal parameters. Then we marked and referenced the 29 target points but they were not considered in the processing. Three well distributed points were used to change from relative to absolute coordinates and the rest of these 29 points were used as check points. The option field calibration was chosen and the IOP were stored. With field calibration 2, we also set an automated project in the same way as with field calibration 1, but 29 natural targets were marked apart from the 29 target points used as GCP and check points. The natural targets were considered for the processing. This field calibration had automatic points and points introduced manually and on field calibration 3 a standard project was used marking and referencing as many targets as we recognised on the images and when the project began to be processed, the option field calibration was chosen. This calibration was carried out only with points introduced manually. The 29 target points were not considered in the processing. The chosen error estimator was the RMS based on the 29 GCPs set. To find out the accuracy of the methods proposed, horizontal and vertical coordinates of the targets points were determined in the ED-50 reference frame with the Ibergeo geoidal model, using a Trimble R6 GPS receiver and applying a post-process method with the Trimble Geomatic Office software. We used the time data correction from the Almeria station, belonging to the Positioning Andalusian Network (RAP).

3. RESULTS

The paper presents the process, the results and the accuracy of these calibration methods. After the software processing, the camera calibration parameters values were obtained.

The calibrated parameters obtained were: focal length, format size of the CCD sensor, location of the principal point sensor, three radial distortion function coefficients and two decentring distortion function coefficients (see table 1, 2, 3 and 4). A high correlation was found with K2 and K3 parameters in all calibrations. This high correlation is normal for radial lens distortion model. Mitishita et.al. (2010) also found a high correlation between radial lens distortions but in this case with K1 and K2. It can be said that radial lens distortion in our work can be modelled by only two parameters (K1 and K2).

	Lab calibration	
Focal length (mm)	8.184 ± 7.8 e-004	
Format size (mm)	7.485 x 5.613	
Principal point (mm)	3.723 ± 8.6 e-004 x 2.677 ± 0.001	
Radial distortion function parameters	K1	2.747e-003 ± 2.6 e-005
	K2	-3.108 e-006 ± 4.0 e-006
	K3	-5.903 e-007 ± 1.9 e-007
Decentring distortion function parameters	P1	5.097 e-005 ± 3.3 e-006
	P2	-4.489 e-004 ± 3.9 e-006

Table 1. Camera lab calibration parameters values

	Field calibration 1	
Focal length (mm)	8.184	
Format size (mm)	7.485 x 5.613	
Principal point (mm)	3.728 ± 0.016 x 2.804 ± 0.017	
Radial distortion function parameters	K1	2.397 e-003 ± 6.8 e-005
	K2	2.270 e-005 ± 6.8 e-006
	K3	-1.951 e-006 ± 2.6 e-007
Decentring distortion function parameters	P1	1.315 e-004 ± 1.1 e-004
	P2	-4.311 e-004 ± 1.0 e-004

Table 2. Camera field calibration 1 parameters values

	Field calibration 2	
Focal length (mm)	8.184	
Format size (mm)	7.485 x 5.613	
Principal point (mm)	3.725 ± 0.014 x 2.803 ± 0.016	
Radial distortion function parameters	K1	2.438 e-003 ± 6.4 e-005
	K2	1.962 e-005 ± 6.3 e-006
	K3	-1.811 e-006 ± 2.4 e-007
Decentring distortion function parameters	P1	1.264 e-004 ± 1.1 e-004
	P2	-4.669 e-004 ± 9.7 e-005

Table 3. Camera field calibration 2 parameters values

	Field calibration 3	
Focal length (mm)	8.184	
Format size (mm)	7.485 x 5.613	
Principal point (mm)	3.720 ± 0.020 x 2.793 ± 0.020	
Radial distortion function parameters	K1	2.611 e-003 ± 7.5 e-005
	K2	-2.907 e-006 ± 6.5 e-006
	K3	-6.916 e-007 ± 2.1 e-007
Decentring distortion function parameters	P1	1.103 e-004 ± 1.4 e-004
	P2	-6.662 e-004 ± 1.1 e-004

Table 4. Camera field calibration 3 parameters values

To review the accuracy of the camera calibration results, the total final error must be checked. Total error is a statistical measure that is calculated in processing. In bundle adjustment it is needed to set a scaling value for all expected parameters precisions. PhotoModeler sets this scale to 1.0. When all assumptions of the adjustment are met, the output should be 1.0 also. This means that the total error value on the last iteration should be 1.0 if everything matches our expectations. When the final total error is less than 1.0, it can be said that the data model (including camera parameters) is good and the marking is more precise than the assumptions. According to Photomodeler (www.photomodeler.com) a value less than 1.0 pixel indicates a good calibration and very good calibrations can have a final total error smaller than 0.4 pixels. In our work, the lab calibration had a final total error of 1.940 pixel (see table 5). It is a total error a bit higher than the recommended to be a good project but the higher error does not necessarily mean the project itself is bad or inaccurate (www.photomodeler.com). The field calibration 1 had a total error of 0.887 pixel, field calibration 2, 0.885 pixel and field calibration 3, 0.565 pixel. The total errors of all field calibration methods are under 1.0 pixel, which is assumed to be a good calibration.

	Final total error (pixel)	**Largest marking residual (pixel)**	**Overall RMS (pixel)**
Lab calibration	1.940	0.723	0.245
Field calibration 1	0.887	3.108	0.721
Field calibration 2	0.885	3.091	0.721
Field calibration 3	0.565	2.738	0.500

Table 5. Total final error and residuals of the camera calibration methods

If the bars in the error chart (see Fig. 4 and Fig. 5) get smaller, the final total error decreases. Also checking the marking residuals is a good way to test the calibration quality. Photomodeler (www.photomodeler.com) recommended having a largest marking residual less than 1.0 pixel. The largest marking residual in lab calibration is less than 1.0 pixel (0.723 pixels). The value of the largest marking residual on field calibration methods are about 3.0 pixels (see table 5), having field calibration 3 better results as field calibration 1 and field calibration 2.

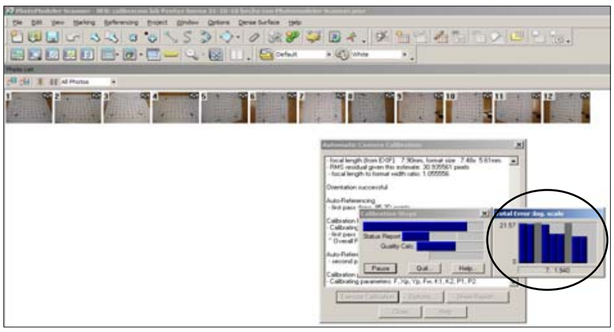

Figure 4. Processing of the lab calibration where the accumulated error can be seen representing by the error chart

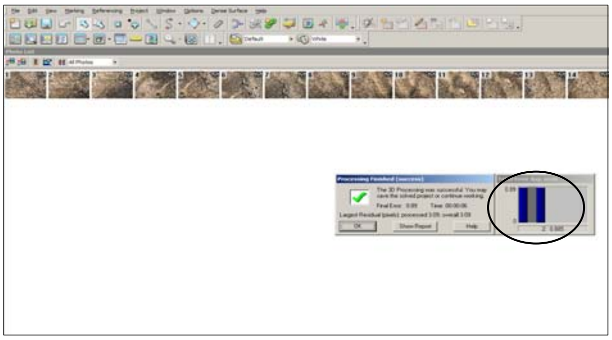

Figure 5. Processing of the field calibration 2 where the accumulated error can be seen representing by the error chart

Accuracy of field calibration was also checked with the error estimator RMS. This software only needs three control points to change from relative to absolute coordinates. For this process the same set of three well distributed control points was chosen on the three field calibration projects. The planimetric and the altimetric RMS were calculated (see table 6). The RMSs obtained had the same magnitude order. These small errors point out the accuracy of the calibration projects.

	Field calibration 1	**Field calibration 2**	**Field calibration 3**
RMS xy	0.191	0.178	0.162
RMS z	0.182	0.174	0.120

Table 6. Planimetric and altimetric RMS of the field calibration methods

4. DISCUSSION

The results in our work show that Photomodeler Scanner software is a powerful and flexible tool for camera calibration using the bundle block adjustment method. Wiggenhagen (2002), Remondino and Fraser (2006), Wotjas (2010), Zhang et al. (2010) and Barazzetti et. al. (2011) also used Photomodeler software to calibrate digital cameras with good results.

The management of Photomodeler Scanner for applying a lab calibration or field calibrations is very straightforward and its relative low-cost in comparison with other photogrammetric software, make it an appropriate software for camera calibration.

The field calibration methods have the advantage that the camera calibration is made in the environmental conditions and the surface to be modelled. Therefore, the use of field calibration might assume a great advance, since the calibration can be done with the same images to use for a final photogrammetric project assuming approximate interior parameters of the camera and then recalibrating the camera with the field calibration option. Clarke and Fryer (1998) also emphasize the advances of field calibration.

Comparing the three field calibration methods, the simplicity of field calibration 1 represents the highest advantage of this technique. This method is less laborious than field calibration 2 and field calibration 3 and all the quality parameters are in the same magnitude order.

The Pentax Optio A40 imagery collected in a flight over 50 m with a md4-200 has demonstrated the potential of high resolution digital imagery for calibration purposes or photogrametric projects.

5. CONCLUSION AND FUTURE WORK

It was concluded that in our photogrammetric applications maybe we can avoid a very strict surveying of GCP to the block adjustment, if we use the automatic autocorrelation algorithm to obtain the tie points. The lab calibration can be carried out once in order to characterize the IOP and then it can be used as pre-calibration in all field calibrations.
Future work will be focusing in the photogrammetric network including rotated photos to check whether the accuracy of the project will be improved, flying over ground at different altitudes and using others digital cameras.
Furthermore, an experimental design will be made which let us to carry out an analysis of the variance, in order to study if the differences between RMS obtained in the three methods are statistically significant.

6. REFERENCES

Barazzetti, L., Binda, L., Scaioni, M. and Taranto, P. 2011. Photogrammetric survey of complex geometries with low-cost software: Application to the 'G1' temple in Myson, Vietnam. *Journal of Cultural Heritage.* 12, pp. 253-262.

Cardenal, J., Mata, E., Castro, P., Delgado, J., Hernández, M. A., Pérez, J. L., Ramos, M. and Torres, M, 2004. Evaluation of a digital non metric camera (Canon D30) for the photogrammetric recording of historical buildings. In: *International Archives of the Photogrammetry, Remote Sensing and Spatial Information Sciences*, Istanbul, Turkey, Vol. 34, Part XXX.

Clarke, T.A. and Fryer J.G. 1998. The development of camera calibration methods and models. *Photogrammetric Record*, 16 (91), pp 51-66.

Colomina, I., Blázquez, M., Molina, P., Parés, M.E. and Wis, M., 2008. Towards a new paradigm for high-resolution low-cost photogrammetry and remote sensing. In: *IAPRS&SIS*, Beijing, China, Vol. 37, Part B1.

Cramer, M. 2004. EuroSDR network on digital camera calibration. In: *International Archives of the Photogrammetry, Remote Sensing and Spatial Information Science.* Istanbul, Turkey, Vol.XXXV, Part A.

Douskos V., Kalisperakis I. and Karras G. 2007. Automatic calibration of digital cameras using planar chess-board patterns. *8th Conf. Opt. 3-D Meas. Techn*., Wichmann, vol. I, pp. 132-140.

Eisenbeiss, H., 2009. UAV photogrammetry. PhD Thesis. ETH Zurich, Switzerland, p. 235.

Fryer, J.G. 1996. Camera calibration. In: *Close Range Photogrammetry and Machine Vision*. K.B. Atkinson Ed., Whittler Publishing, Caithness, pp. 156-179.

Grammatikopoulos L., Karras G. and Petsa E. 2007. An automatic approach for camera calibration from vanishing points*. ISPRS Journal of Photogrammetry and Remote Sensing*, vol. 62, pp. 64-76.

Gruen, A. and Akca, D., 2008. Metric accuracy testing with mobile phone cameras. In: *The International Archives of the Photogrammetry, Remote Sensing and Spatial Information Sciences*, Beijing, China, Vol. XXXVII, Part B5, pp. 729–736.

Habib, A.F. and Morgan, M.F. 2003. Automatic calibration of low-cost digital cameras. *Opt. Eng.* 42, pp. 948-955.

Honkavaara, E., Ahokas, E. Hyyppä, J., Jaakkola, J., Kaartinen, H., Kuittinen, R., Markelin, L. and Nurminen, K. 2006. Geometric test field calibration of digital photogrammetric sensors. *ISPRS Journal of Photogrammetry & Remote Sensing.* 60, pp. 387–399.

Irschara, A., Kaufmann, V., Klopschitz, M., Bischof, H. and Leberl, F. 2010. Towards fully automatic photogrammetric reconstruction using digital images taken from UAVs. In: *International Archives of the Photogrammetry, Remote Sensing and Spatial Information Sciences,* Vienna, Austria, Vol. XXXVIII, Part 7A, pp. 65-70.

Karras, G.E. and Mavrommati, D. 2001. Simple calibration techniques for non-metric cameras. In: *CIPA International Symposium*, Potsdam, Germany, pp. 18-21.

Mason, S., Rüther, H. and Smit, J. 1997. Investigation of the Kodak DCS460 digital camera for small-area mapping. *ISPRS Journal of Photogrammetry & Remote Sensing,* 52, pp. 202-214.

Microdrones GmbH website.
http://www.microdrones.com/en_home.php (27 Oct. 2011)

Mitishita, E., Cortes, J., Centeno, J., Machado, A. and Martins, M. 2010. In: *International Archives of the Photogrammetry, Remote Sensing and Spatial Information Sciences*, Calgary, Canada, Vol XXXVIII, part 1.

Photomodeler software website.
http://www.photomodeler.com. (27 Oct. 2011)

Positioning Andalusian Network (RAP) website.
http://www.juntadeandalucia.es/obraspublicasytransportes/redandaluzadeposicionamiento/rap. (31 June 2010)

Remondino F. and Fraser C. 2006. Digital camera calibration methods: considerations and comparisons. In: *International Archives of Photogrammetry, Remote Sensing and Spatial Information Sciences*, Vol. XXXVI, part 5, pp. 266-272.

Wang, J., Shi, F., Zhang, J. and Liu, Y. 2008. A new calibration model of camera lens distortion, *Pattern Recognition*, vol. 41, pp. 607–615.

Warner W. S. and Carson, W.W. 1991. Improving Interior Orientation for a Small Standard Camera. *Photogrammetric Record*. 13(78), pp. 909-916.

Wiggenhagen, M. 2002. Calibration of Digital Consumer Cameras for Photogrammetric Applications, In: *International Archives of Photogrammetry, Remote Sensing and Spatial Information Sciences*, Graz, Austria, Vol XXXIV, part B, pp. 301-304.

William, K. 2005. Digital vertical aerial camera system for high-resolution site inspections in conservation easement monitoring. PhD Thesis. University of Maine. EEUU. p. 161.

Wotjas, A.M. 2010. Off the self close range photogrammetric software for cultural heritage documentation at Stonehenge. *International Archives of Photogrammetry, Remote Sensing and Spatial Information Sciences,* Vol. XXXVIII. 603-607.

Zhang, Z. 2000. A flexible new technique for camera calibration*, IEEE Trans. Pattern Anal. Mach. Intell*. 22 (11) pp. 1330–1334.

Zhang, W., Jiang, T. and Han, M. 2010. Digital camera calibration method based on PhotoModeler. *3rd International Congress on Image and Signal Processing* (CISP2010), pp. 1235-1238.

7. ACKNOWLEDGEMENTS

This work was supported by grand P08-TEP-3870 from CICE-Junta de Andalucía (Spain), co-financed with FEDER funds of the European Union.